



Composition of the Earth's inner core from high-pressure sound velocity measurements in Fe–Ni–Si alloys

Daniele Antonangeli^{a,b,*}, Julien Siebert^{a,b}, James Badro^{a,b}, Daniel L. Farber^{b,c}, Guillaume Fiquet^a, Guillaume Morard^a, Frederick J. Ryerson^b

^a Institut de Minéralogie et de Physique des Milieux Condensés, UMR CNRS 7590, Institut de Physique du Globe de Paris, Université Pierre et Marie Curie, Université Paris Diderot, 75005 Paris, France

^b Lawrence Livermore National Laboratory, Livermore, CA 94550, USA

^c Department of Earth and Planetary Sciences, University of California, Santa Cruz, Santa Cruz, CA, 95064, USA

ARTICLE INFO

Article history:

Received 16 November 2009

Received in revised form 7 April 2010

Accepted 10 April 2010

Available online 10 May 2010

Editor: R.D. van der Hilst

Keywords:

Fe–Ni–Si alloy

aggregate compressional and shear sound velocities

high pressure

inner core

light elements

ABSTRACT

We performed room-temperature sound velocity and density measurements on a polycrystalline alloy, Fe_{0.89}Ni_{0.04}Si_{0.07}, in the hexagonal close-packed (hcp) phase up to 108 GPa. Over the investigated pressure range the aggregate compressional sound velocity is ~9% higher than in pure iron at the same density. The measured aggregate compressional (V_P) and shear (V_S) sound velocities, extrapolated to core densities and corrected for anharmonic temperature effects, are compared with seismic profiles. Our results provide constraints on the silicon abundance in the core, suggesting a model that simultaneously matches the primary seismic observables, density, P-wave and S-wave velocities, for an inner core containing 4 to 5 wt.% of Ni and 1 to 2 wt.% of Si.

© 2010 Elsevier B.V. All rights reserved.

1. Introduction

The study of seismic wave propagation and normal mode oscillation are, without doubt, two of the most direct probes of the Earth's interior, providing a remote sensing method to obtain sound velocities and density. However, to derive an accurate compositional model, these seismic observations have to be combined with laboratory-based experiments constraining the density and elastic properties of highly compressed minerals. Based on shock wave measurements, Birch proposed in the early 1950's that the Earth's core was mainly composed of iron alloyed with nickel and some "light element(s)", required to account for the observed density difference between the core and pure iron (Birch, 1952). Since then, a large number of experimental and theoretical studies addressed the nature and concentration of these light elements (see review by Poirier (Poirier, 1994)), with several elements proposed. Geo- and cosmochemical arguments suggest that most likely candidates are sulfur (Williams and Jeanloz, 1990; Sherman, 1991;

Sherman, 1995; Sherman, 1997; Li et al., 2001; Vočadlo, 2007; Morard et al., 2008; Côté et al., 2008a), oxygen (Sherman, 1991; Sherman, 1995; Stixrude et al., 1997; Rubie et al., 2004; Badro et al., 2007; Asahara et al., 2007; Corgne et al., 2009), and silicon (Sherman, 1997; Dobson et al., 2003; Vočadlo, 2007; Badro et al., 2007; Côté et al., 2008a; Côté et al., 2008b; Asanuma et al., 2008). Very recently, high-pressure measurements of sound velocity and density of several iron compounds (FeO, FeSi, FeS, and FeS₂) in conjunction with data on pure iron, pointed out inconsistencies when considering sulfur as the only major light element, and proposed an Earth's inner core composed of iron alloyed with silicon (2.3 wt.%) and traces oxygen (0.1 wt.%) (Badro et al., 2007). However, these results are based on three primary assumptions:

- a linear dependence of compressional sound velocity (V_P) on density ("Birch's law");
- the P-wave velocity of the alloy is equal to a geometrical average of that of the minor compound and the metal (*i.e.* ideal mixing behavior); and
- the inclusion of up to 5 wt.% Ni has a negligible effect on sound velocity.

Further, a clear limitation of this model is that only the aggregate compressional sound velocity was taken into account, whereas the largest discrepancy between the seismological observations and the

* Corresponding author. Institut de Minéralogie et de Physique des Milieux Condensés, UMR CNRS 7590, Institut de Physique du Globe de Paris, Université Pierre et Marie Curie, Université Paris Diderot, 75005 Paris, France.

E-mail address: daniele.antonangeli@impmc.upmc.fr (D. Antonangeli).

results from molecular dynamics simulations and diamond anvil experiments is observed for the shear wave velocity (Deuss, 2008).

Therefore, in order to validate the overall proposed model of the core composition, as well as to address the legitimacy and the possible limits of the adopted approximations, we undertook an experimental investigation of (Fe, Ni, Si) alloy samples. Specifically, we carried out sound velocity and density measurements on polycrystalline samples containing 4.3 wt.% of Ni and 3.7 wt.% of Si, compressed in diamond anvil cell (DAC) to megabar pressures. Details of sample synthesis and characterization, as well as of the inelastic X-ray scattering (IXS) measurements are reported in the next section, while the obtained results are illustrated and discussed in Section 3. Our main conclusions are summarized in Section 4.

2. Experimental details

Polycrystalline homogeneous samples of silicon bearing iron–nickel alloy have been prepared at high pressure and high temperature. Partial oxidation of silicon metal is a critical issue in the synthesis of silicon-rich iron alloy. The experiment has been conducted at superliquidus conditions to segregate from a SiO₂ glass a (Fe, Ni, Si) metallic blob free of SiO₂ inclusions. The starting material consisted in homogenized mixture of high purity metallic and oxide powders of Fe, Si, Ni and SiO₂, with a 60 wt.% metallic portion relative to oxide. Piston cylinder experiment was carried out at 10 kbars and 1850 °C at the Lawrence Livermore National Laboratory, using a standard 1/2" BaCO₃ pressure cell assembly, with a graphite furnace and a MgO capsule. The recovered metallic blob of about 1 mm diameter was analyzed with an electron probe micro-analyzer operating at 20 kV and 50 nA. Multiple analyses as well as backscattered electron images show homogenous (Fe, Ni, Si) alloy composition without quench textures at least at the scale of imaging and analytical resolution. Silicon and nickel concentrations are 3.7 wt.% and 4.3 wt.%, respectively.

Compacted pellets of about 90 μm in diameter and 20 μm thick were loaded in DACs equipped with Re gasket, using 300 μm flat anvils and neon as pressure transmitting medium for measurements up to 50 GPa, and 150/300 μm beveled anvils with no pressure transmitting medium for higher pressures. Pressures were determined by ruby fluorescence and, most importantly, the densities (ρ) were directly obtained from diffraction measurements and cross-checked with the equation of state previously measured on the same samples (Fiquet et al., 2008).

Inelastic X-ray scattering measurements were carried out on the ID28 beamline at the European Synchrotron Radiation Facility, using the Si(8,8,8) instrument configuration, which provides the best compromise between flux and energy resolution (5.5 meV full width half maximum, FWHM) for polycrystalline samples compressed in DAC. Spectra have been collected in transmission geometry, with the X-ray beam impinging on the sample through the diamonds, along the main compression axis of the cell, and hence probing exchange momenta *q* almost perpendicular to the cell-axis. The transverse dimensions of the focused X-ray beam of 30 × 90 μm² (horizontal X vertical, FWHM) were further reduced by slits on the vertical direction. Momentum resolution was set to 0.25 nm⁻¹. Further details of the experimental setup can be found elsewhere (Krisch, 2003; Antonangeli et al., 2004a; Antonangeli et al., 2005). By scanning the scattering angle at the elastic energy (*i.e.* *q*-scan at Δ*E* = 0) we collected the [100], [002] and [101] reflections out of our sample, with the momentum resolution of 0.06 nm⁻¹ set by slits in front of the analyzer.

We collected data in the hexagonal close-packed (hcp) phase, at 27, 37 and 47 GPa on quasi-hydrostatically compressed samples, and at 32, 68 and 108 GPa on non-hydrostatically compressed samples. At each investigated pressure point, we mapped the longitudinal acoustic phonon dispersion throughout the entire first Brillouin

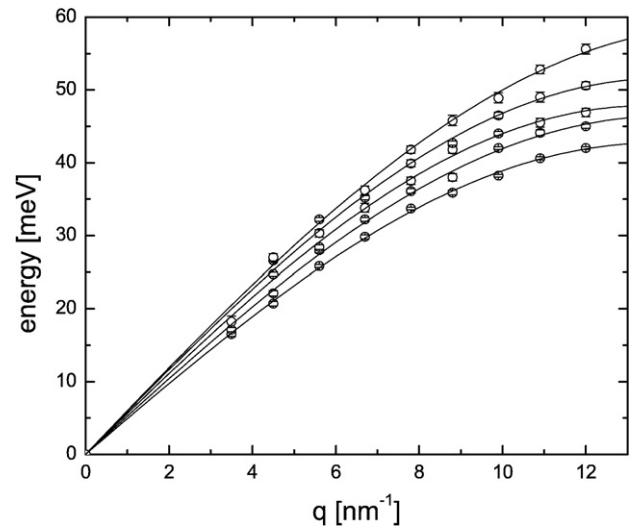


Fig. 1. Longitudinal acoustic phonon dispersion of Fe_{0.89}Ni_{0.04}Si_{0.07} at ambient temperature and pressures of 27, 37, 47, 68 and 108 GPa (bottom to top). For clarity the dispersion at 32 GPa is not plotted. The lines are sine fits to the experimental data.

zone collecting 8–9 spectra in the range of 3.5–12 nm⁻¹ (Fig. 1). The energy positions of the phonons were extracted by fitting a set of Lorentzian functions convolved with the experimental resolution function to the IXS spectra, utilizing a standard χ^2 minimization routine. We then derived the aggregate compressional sound velocity V_P from a sine fit (Born–von Karman lattice-dynamics theory limited to 1st neighbor interaction) to the phonon dispersion (Antonangeli et al., 2004a; Antonangeli et al., 2005), with error bars between ± 2 and $\pm 3\%$ (Fig. 1). Combining our measurements of V_P and ρ with the values of bulk modulus, *K* (Fiquet et al., 2008), we also obtained the aggregate shear sound velocities V_S from the relation $V_S = [3/4 (V_P^2 - K/\rho)]^{1/2}$, although with larger uncertainty (± 4 –6%) due to error propagation.

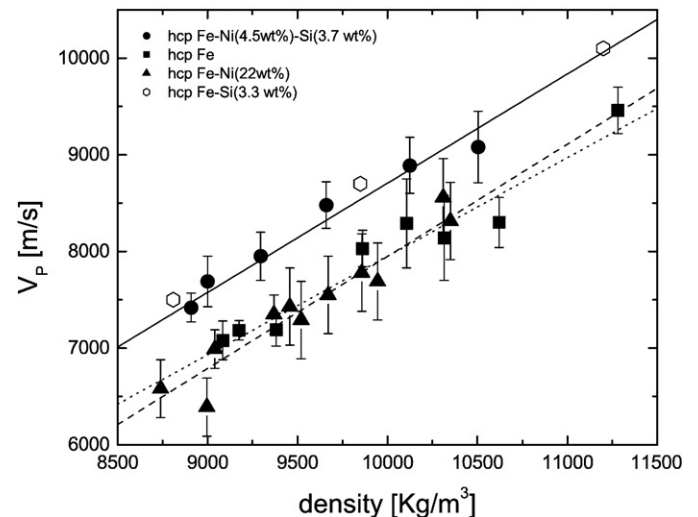


Fig. 2. Aggregate compressional sound velocity as a function of density. Circles: Fe_{0.89}Ni_{0.04}Si_{0.07}; squares: Fe (Fiquet et al., 2001; Antonangeli et al., 2004a); triangles: Fe_{0.78}Ni_{0.22} (Kantor et al., 2007); open hexagons: computational results on Fe_{0.9375}Si_{0.0625} (Tsuchiya and Fujibuchi, 2009). The displayed error bars of the velocities result from the experimental uncertainties, the statistical error of the fit, and the finite-*q* resolution of the spectrometer. The uncertainties in the densities are smaller than the symbols. Lines are linear regressions to the experimental data (solid – Fe_{0.89}Ni_{0.04}Si_{0.07}; dotted – Fe; dashed – Fe_{0.78}Ni_{0.22}).

3. Results and discussion

The measured compressional sound velocities are plotted as a function of density in Fig. 2, together with values for pure iron (Fiquet et al., 2001; Antonangeli et al., 2004a) and Fe_{0.78}Ni_{0.22} alloy (Kantor et al., 2007). To provide an analysis unbiased by systematic differences resulting from different techniques, pressure scales or approximations in the equation of state, and thus to be able to resolve variations as low as a few percent, we have only considered data obtained by IXS for conditions where the density was directly measured. While no systematic offsets can be observed between data for pure iron and iron–nickel alloy, our velocity measurements for Fe_{0.89}Ni_{0.04}Si_{0.07} are systematically higher, as highlighted by the linear fits to the experimental data (Fig. 2). Over the investigated pressure range, Fe_{0.89}Ni_{0.04}Si_{0.07} is approximately 9% faster than pure iron at the same density. We also note that our experimental results compare favourably with calculations on Fe_{0.9375}Si_{0.0625} (Tsuchiya and Fujibuchi, 2009) (Fig. 2), further stressing that the increase in the sound velocity is solely due to the silicon incorporation with no observable effect due to nickel.

To compare directly with seismic models however, our results need to be extrapolated to core conditions. Within the experimental uncertainties, all the datasets exhibit a linear dependence of V_P with density (*i.e.* follow “Birch’s law”), as also observed in several other high-pressure experimental and theoretical studies (Vočadlo, 2007; Badro et al., 2007; Kantor et al., 2007; Antonangeli et al., 2008; Tsuchiya and Fujibuchi, 2009). Hence, as a first approximation (see discussion later on), within a quasi-harmonic limit, we assume a linear dependence of the compressional sound velocities with density, irrespective of the specific pressure and temperature conditions.

Also, since we are interested in the isotropic aggregate properties, we carefully checked our data for preferential alignment and elastic anisotropy. In the case of non-hydrostatically compressed iron, angular dependence of V_P has been documented starting above ~80 GPa (Antonangeli et al., 2004a), as a combined effect of the deformation-related development of preferred orientation and of the intrinsic single-crystalline elastic anisotropy. Preferential alignment of the *c*-axis along the main compression axis of the cell has been observed for several hcp metals when compressed uniaxially (Wenk et al., 2000; Merkel et al., 2004; Merkel et al., 2006). Hence, we compared the relative intensities of the [100], [002] and [101] reflections and the *c/a* ratio obtained under hydrostatic conditions using Ne as pressure transmitting medium with those obtained under non-hydrostatic conditions. While all the diffraction patterns collected from hydrostatically compressed samples show no significant variation on the intensities with increasing pressure, the intensity of the [002] reflection exhibits a strong reduction upon compression and almost vanishes at pressures exceeding 30 GPa, for samples loaded without pressure transmitting medium. Such behavior is expected for the utilized diffraction geometry as a consequence of the progressive alignment of the crystalline *c*-axis with the main compression axis of the cell. However, the volumes and the values for *c/a* derived solely from the [100] and [101] reflections did not significantly differ from those obtained under quasi-hydrostatic compression up to ~90 GPa. Conversely, the volume derived at 108 GPa is quite different from expected according to the quasi-hydrostatic equation of state (Fiquet et al., 2008) and the *c/a* ratio displays a large deviation. Deviation of individual d-spacings from the values expected in the limit of hydrostatic compression is a direct consequence of the presence of a deviatoric stress within the cell, and if the strain $\epsilon_{hkl} = (d_{hkl} - d_{hkl}^{hydro}) / d_{hkl}^{hydro}$ for all the lattice planes is the same for elastically isotropic materials, this is not the case in the presence of elastic anisotropy (see for instance Singh et al., 1998; Merkel et al., 2009). Thus, we can conclude that all our non-hydrostatic pressure points ($P \sim 32, 68$ and 108 GPa) exhibit some texture, but a significant

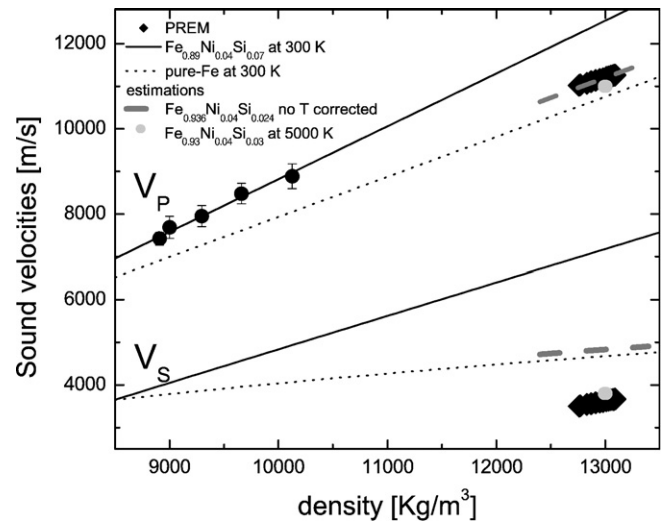


Fig. 3. Aggregate compressional (V_P) and shear (V_S) sound velocities and density extrapolations (considering only data up to 68 GPa). Circles: IXS data on Fe_{0.89}Ni_{0.04}Si_{0.07}; diamonds: PREM (Dziewonski and Anderson, 1981). Solid lines – Fe_{0.89}Ni_{0.04}Si_{0.07}; dotted lines – pure Fe (Badro et al., 2007). V_S has been derived combining the measured V_P with literature equation of state (Fe_{0.89}Ni_{0.04}Si_{0.07}: (Fiquet et al., 2008); Fe: (Dewaele et al., 2006)). Gray dashes are our estimated values of V_P and V_S for Fe_{0.89}Ni_{0.04}Si_{0.07} (Si content ~1.2 wt.%), neglecting temperature corrections. Light gray dots are our estimated values of V_P and V_S for Fe_{0.9375}Si_{0.0625} (Si content ~1.5 wt.%) at 13,000 Kg/m³ and 5000 K. For clarity uncertainties in our estimations (about $\pm 3\%$ for V_P and $\pm 10\%$ for V_S , without temperature corrections, and about $\pm 5\%$ for V_P and $\pm 12\%$ for V_S when considering temperature corrections) are not reported.

deviation from a radially averaged sound velocity is observed only at 108 GPa. To support this conclusion, we note that as a direct consequence of the developed preferential alignment and the predominant contribution of the slow-velocity basal plane (Antonangeli et al., 2004a; Antonangeli et al., 2004b; Antonangeli et al., 2006; Mao et al., 2008), the V_P value at the highest density (highest pressure) is somewhat lower than the linear trend, although still within uncertainties (Fig. 2).

Due to the deviation from radial average properties at the highest pressures, we only considered data up to 68 GPa for extrapolation of V_P and V_S to core conditions. Our results are reported in Fig. 3 along with linear regressions and the density evolution proposed for pure Fe (Badro et al., 2007), and compared with the seismic velocity profile from the radial PREM model for the inner core (Dziewonski and Anderson, 1981). As already suggested (Fiquet et al., 2001; Badro et al., 2007), V_P for pure hcp-Fe is somewhat lower than the PREM; this study shows that adding 3.7 wt.% Si yields a velocity that is too fast relative to PREM (Fig. 3). If we consider linear mixing of pure Fe and Fe_{0.89}Ni_{0.04}Si_{0.07} (assuming an ideal two-component solid solution (Badro et al., 2007)), we simultaneously match the PREM values of V_P and ρ for an alloy with 1.2 wt.% of Si (gray dashes in Fig. 3).

Considering V_S increases the complexity of the problem. Both Fe and Fe_{0.89}Ni_{0.04}Si_{0.07} exhibit values of shear velocities¹ significantly higher than PREM (Fig. 3). The mismatch for Fe_{0.89}Ni_{0.04}Si_{0.07} is even larger than for pure iron. Indeed, inclusion of silicon leads to a much larger increase in V_S than in V_P , due to a smaller pressure derivative of the bulk modulus (K') that is only partially balanced by a larger value of K_0 . As a result, Fe_{0.89}Ni_{0.04}Si_{0.07} has a larger pressure derivative for V_S than pure Fe, which manifests itself as a considerable divergence between the data sets when extrapolated to core densities. Using this model, it is clear that we cannot simultaneously solve for V_P , V_S and ρ of the core by simply varying the amounts of Ni and Si or pressure.

¹ Extrapolated values of V_S are obtained assuming the Birch’s law to be valid for both V_P and $V_b = (K/\rho)^{1/2}$. The resulting V_S exhibits a sub-linear dependence on density.

At core temperatures (4000–6000 K) anharmonic effects are expected. These might be particularly relevant to V_S , as already pointed by computational studies (Laio et al., 2000; Steinle-Neumann et al., 2001), that suggest significantly lower values of V_S as temperature approaches the melting point. As such, we applied temperature corrections to our ambient temperature results. Very recent *ab initio* calculations on hcp iron (Vočadlo et al., 2009) suggest about 9.5% and about 35% softening for V_P and V_S respectively, between 0 and 5000 K. Such a temperature increase yields a density reduction about 4%. Since we are interested in only the anharmonic high temperature effects (we are comparing data at the same density), we corrected these computational results according to the measured density dependence of sound velocities to compensate for the density variation, obtaining 4% softening of V_P and 30% softening of V_S at 5000 K and 13,000 Kg/m³. The thermal softening of V_P at constant density requires an increase in the Si content to ~1.5 wt.% in order to match the seismic observations. Most importantly, this composition appears to provide a simultaneous solution for both V_P and V_S , consistent with PREM values (light gray dots in Fig. 3).

4. Conclusions

Our new sound velocity and density measurements on hcp Fe_{0.89}Ni_{0.04}Si_{0.07} polycrystalline samples compressed in DAC to 108 GPa yield values of V_P that are about 9% higher than in pure iron (at the same density). As it has already been shown that alloying with Ni does not significantly influence the elastic properties of Fe, at least up to a concentration of 22 at.% (Kantor et al., 2007), we can reasonably assume that the increase in the sound velocity is solely due to the presence of Si. This conclusion is further supported by comparison of our measurements with computational results on Fe_{0.9375}Si_{0.0625} (Tsuchiya and Fujibuchi, 2009).

Extrapolation to core densities and comparison with seismic velocity and density profiles from PREM allow us to constrain compositional models of the core. Our results suggest an inner core composition containing 4–5 wt.% of Ni and 1–2 wt.% of Si. The exact amount of Si might vary depending upon the temperature corrections (here we used values calculated for pure Fe), or if other elements are also present in the inner core. The approximations in our model and the relatively large uncertainties, especially on V_S , do not allow us to definitively rule out other compositional models, and other light elements might be present in amount below our present limit of sensitivity (~1 wt.%). It should be noted that our conclusions pertain strictly to solid Fe-alloys and hence the inner core. Elements such as oxygen, that may be incompatible in solid relative to liquid Fe-alloys, are expected to reside mainly in the outer core (see for instance (Alfe et al., 2002; Badro et al., 2007)) and cannot be adequately constrained here. Furthermore, given the negligible influence of nickel on the elastic properties, we fixed the Ni content according to the abundance considered in common cosmochemical models (see for instance Poirier, 1994). However, our proposed core composition is consistent with existing experimental data and, for the first time, simultaneously matches all three primary geophysical observables (V_P , V_S and ρ). Combined with Si partition coefficients between liquid and solid Fe we can estimate the Si concentration of the liquid outer core and, hence, obtain a Si concentration for the entire core. If we assume a molar partition coefficient for silicon between the liquid and solid phase of iron of $1.2 \leq D^{\text{Liq/Sol}} \leq 1.9$ (Alfe et al., 2002), we obtain a core composition with Si ranging from 1.2 to 4 wt.%, for an inner core containing 1 to 2 wt.% of Si. This result is at the lower range of those from core-formation and core–mantle interaction models that often call for large amount of Si in the core (e.g. 7.3 wt.% (Allègre et al., 1995), 10.3 wt.% (Javoy, 1995), and 5–7 wt.% (Wade and Wood, 2005)).

Several mechanisms have been proposed to explain the low shear velocity in the core, including fluid inclusions (Singh et al., 2000;

Vočadlo, 2007), viscoelastic relaxation (Jackson et al., 2000) or the presence of randomly oriented anisotropic “patches” (Calvet and Margerin, 2008). According to our present results, none of these is strictly necessary, and V_P and V_S can be matched, although with some uncertainties due to the discussed approximations, by only considering the effect of alloying silicon at the few wt.% level with reasonable high temperature anharmonic corrections inferred from recent theoretical calculations (Vočadlo et al., 2009). However, the above-mentioned possibilities (Singh et al., 2000; Vočadlo, 2007; Jackson et al., 2000; Calvet and Margerin, 2008) become relevant to reconciliation of observed seismic wave attenuation. In addition, seismic anisotropy, its variation with depth, as well core hemisphericity, require higher complexity than the simple radial model discussed here.

Acknowledgment

We acknowledge the European Synchrotron Radiation facility for provision of beamtime and we thank M. Hoesch and M. Krisch for assistance on ID 28. C. Aracne and D. Ruddle are acknowledged for technical support, P. Munsch and G. Le Marchande for gas loading. We wish to thank L. Vočadlo for sharing unpublished results. This work was supported by the French National Research Agency (ANR) grant no. ANR-07-BLAN-0124-01, and also performed under the auspices of the U.S. Department of Energy, Lawrence Livermore National Laboratory under Contract DE-AC52-07NA27344, supported by the Office of Basic Energy Sciences (FJR), and the Laboratory Directed Research and Development Program at IGPP/LLNL (JS). J. Badro acknowledges financial support from the European Community's Seventh Framework Programme (FP7/2007–2013)/ERC grant agreement no. 207467.

References

- Alfe, D., Gillan, M.J., Price, G.D., 2002. Composition and temperature of the Earth's core constrained by combining *ab initio* calculations and seismic data. *Earth Planet. Sci. Lett.* 195, 91–98.
- Allègre, C.J., Poirier, J.P., Humler, E., Hofman, A., 1995. The chemical composition of the Earth. *Earth Planet. Sci. Lett.* 134, 515–526.
- Antonangeli, D., Ocellli, F., Requardt, H., Badro, J., Fiquet, G., Krisch, M., 2004a. Elastic anisotropy in textured hcp-iron to 112 GPa from sound wave propagation measurements. *Earth Planet. Sci. Lett.* 225, 243–251.
- Antonangeli, D., Krisch, M., Fiquet, G., Farber, D.L., Aracne, C., Badro, J., Ocellli, F., Requardt, H., 2004b. Elasticity of cobalt at high pressure studied by inelastic X-ray scattering. *Phys. Rev. Lett.* 93, 215505.
- Antonangeli, D., Krisch, M., Fiquet, G., Badro, J., Farber, D.L., Bossak, A., Merkel, S., 2005. Aggregate and single-crystalline elasticity of hcp cobalt at high pressure. *Phys. Rev. B* 72, 134303.
- Antonangeli, D., Merkel, S., Farber, D.L., 2006. Elastic anisotropy in hcp metals at high pressure and the sound wave anisotropy of the Earth's inner core. *Geophys. Res. Lett.* 33, L24303.
- Antonangeli, D., Krisch, M., Farber, D.L., Ruddle, D.G., Fiquet, G., 2008. Elasticity of hexagonal-closed-packed cobalt at high pressure and temperature: a quasiharmonic case. *Phys. Rev. Lett.* 100, 085501.
- Asanuma, H., Ohtani, E., Sakai, T., Terasaki, H., Kamada, S., Hirao, N., Sata, N., Ohishi, Y., 2008. Phase relations of Fe–Si alloy up to core conditions: implications for the Earth inner core. *Geophys. Res. Lett.* 35, L12307.
- Asahara, Y., Frost, D.J., Rubie, D.C., 2007. Partitioning of FeO between magnesiowüstite and liquid iron at high pressures and temperatures: implications for the composition of the Earth's outer core. *Earth Planet. Sci. Lett.* 257, 435–449.
- Badro, J., Fiquet, G., Guyot, F., Gregoryanz, E., Ocellli, F., Antonangeli, D., d'Astuto, M., 2007. Effect of light elements on the sound velocity of solid iron: implications for the composition of Earth's core. *Earth Planet. Sci. Lett.* 254, 233–238.
- Birch, F., 1952. Elasticity and constitution of the Earth's interior. *J. Geophys. Res.* 57, 227–286.
- Calvet, M., Margerin, L., 2008. Constraints on grain size and stable iron phases in the uppermost inner core from multiple scattering modeling of seismic velocity and attenuation. *Earth Planet. Sci. Lett.* 267, 200–212.
- Corgne, A., Siebert, J., Badro, J., 2009. Single-stage formation in a magma ocean requires some oxygen in the core. *Earth Planet. Sci. Lett.* 288, 108–114.
- Côté, A.S., Vočadlo, L., Brodholt, J.P., 2008a. Light elements in the core: effects of impurities on the phase diagram of iron. *Geophys. Res. Lett.* 35, L05306.
- Côté, A.S., Vočadlo, L., Brodholt, J.P., 2008b. The effect of silicon impurities on the phase diagram of iron and possible implications for the Earth's core structure. *J. Phys. Chem. Solids* 69, 2177–2181.

- Dewaele, A., Loubeyre, P., Occelli, F., Mezouar, M., Dorogokupets, P.I., Torrent, M., 2006. Quasihydrostatic equation of state of iron above 2 Mbar. *Phys. Rev. Lett.* 97, 215504.
- Deuss, A., 2008. Normal mode constraints on shear and compressional wave velocity of the Earth's inner core. *Earth Planet. Sci. Lett.* 268, 364–375.
- Dobson, D.P., Crichton, W.A., Bouvier, P., Vočadlo, L., Wood, I.G., 2003. The equation of state of CsCl-structured FeSi to 40 GPa: implications for silicon in the Earth's core. *Geophys. Res. Lett.* 30, 1014.
- Dziewonski, A.M., Anderson, D.L., 1981. Preliminary reference Earth model. *Phys. Earth Planet. Inter.* 25, 297–356.
- Fiquet, G., Badro, J., Guyot, F., Requardt, H., Krisch, M., 2001. Sound velocities in iron to 110 gigapascals. *Science* 291, 468–471.
- Fiquet, G., Boulard, E., Auzende, A., Antonangeli, D., Badro, J., Morard, G., Siebert, J., Perrillat, J., Mezouar, M., 2008. Phase relations of Fe–Si–Ni alloys at core conditions: implications for the Earth inner core. *Eos Trans. AGU* 89 (53) Fall Meet. Suppl., Abstract D153B-08.
- Jackson, I., Gerald, J.F., Kokkonen, H., 2000. High-temperature viscoelastic relaxation in iron and its implications for the shear modulus and attenuation of the Earth's inner core. *J. Geophys. Res.* 1105, 23605–23634.
- Javoy, M., 1995. The integral enstatite chondrite model of the Earth. *Geophys. Res. Lett.* 22, 2219–2222.
- Kantor, A.P., Kantor, I.Y., Kurnusov, A.V., Kuznetsov, A.Y., Dubrovinskaia, N.A., Krisch, M., Bossak, A.A., Dmitriev, V.P., Urusov, V.S., Dubrovinsky, L.S., 2007. Sound wave velocities of fcc Fe–Ni alloy at high pressure and temperature by mean of inelastic X-ray scattering. *Phys. Earth Planet. Inter.* 164, 83–89.
- Krisch, M., 2003. Status of phonon studies at high pressure by inelastic X-ray scattering. *J. Raman Spectrosc.* 34, 628–632.
- Laio, A., Bernard, S., Chiarotti, G.L., Scandolo, S., Tosatti, E., 2000. Physics of iron at Earth's core conditions. *Science* 287, 1027–1030.
- Li, J., Fei, Y., Mao, H.K., Hirose, K., Shieh, S.R., 2001. Sulfur in the Earth's inner core. *Earth Planet. Sci. Lett.* 193, 509–514.
- Mao, W.L., Struzhkin, V.V., Baron, A.Q.R., Tsutsui, S., Tommaseo, C.E., Wenk, H.R., Hu, M.Y., Chow, P., Sturhahn, W., Shu, J., Hemley, R.J., Heinz, D.L., Mao, H.K., 2008. Experimental determination of the elasticity of iron at high pressure. *J. Geophys. Res.* 113, B09213.
- Merkel, S., Wenk, H.R., Gillet, P., Mao, H.K., Hemley, R.J., 2004. Deformation of polycrystalline iron up to 30 GPa and 1000 K. *Phys. Earth Planet. Inter.* 145, 239–251.
- Merkel, S., Miyajima, N., Antonangeli, D., Fiquet, G., Yagi, T., 2006. Lattice preferred orientation and stress in polycrystalline hcp-Co plastically deformed under high pressure. *J. Appl. Phys.* 100, 023510.
- Merkel, S., Tomé, C., Wenk, H.K., 2009. Modeling analysis of the influence of plasticity on high pressure deformation of hcp-Co. *Phys. Rev. B* 79, 064110.
- Morard, G., Andrault, D., Guignot, N., Sanloup, C., Mezouar, M., Petitgirard, S., Fiquet, G., 2008. In-situ determination of Fe–Fe₃S phase diagram and liquid structural properties up to 65 GPa. *Earth Planet. Sci. Lett.* 272, 620–626.
- Poirier, J.P., 1994. Light elements in the Earth's outer core – a critical review. *Phys. Earth Planet. Inter.* 85, 319–337.
- Rubie, D.C., Gessmann, C.K., Frost, D.J., 2004. Partitioning of oxygen during core formation on the Earth and Mars. *Nature* 429, 58–61.
- Sherman, D.M., 1991. Chemical bonding in the outer core: high pressure electronic structures of oxygen and sulfur in metallic iron. *J. Geophys. Res.* 96, 18029–18036.
- Sherman, D.M., 1995. Stability of possible Fe–FeS and Fe–FeO alloy phases at high pressure and the composition of the Earth's core. *Earth Planet. Sci. Lett.* 132, 87–98.
- Sherman, D.M., 1997. The composition of the Earth's core: constraints on S and Si vs. temperature. *Earth Planet. Sci. Lett.* 153, 149–155.
- Singh, A.K., Mao, H.K., Shu, J., Hamley, R.J., 1998. Estimation of the single-crystal elastic moduli from polycrystalline X-ray diffraction at high pressure: application to FeO and iron. *Phys. Rev. Lett.* 80, 2157–2160.
- Singh, S.C., Taylor, M.A.J., Montagner, J.P., 2000. On the presence of liquid in the Earth's inner core. *Science* 287, 2471–2472.
- Steinle-Neumann, G., Stixrude, L., Cohen, R.E., Gülseren, O., 2001. Elasticity of iron at the temperature of the Earth's inner core. *Nature* 413, 57–60.
- Stixrude, L., Wasserman, E., Cohen, R.E., 1997. Composition and temperature of Earth's inner core. *J. Geophys. Res.[Solid Earth]* 102, 24729–24739.
- Tsuchiya, T., Fujibuchi, M., 2009. Effects of Si on the elastic property of Fe at Earth's inner core pressures: first principle study. *Phys. Earth Planet. Inter.* 174, 212–219.
- Vočadlo, L., 2007. Ab initio calculations of the elasticity of iron and iron alloys at inner core conditions: evidence of partially molten core? *Earth Planet. Sci. Lett.* 254, 227–232.
- Vočadlo, L., Dobson, D.P., Wood, I.G., 2009. Ab initio calculations of the elasticity of hcp-Fe as a function of temperature at inner-core pressure. *Earth Planet. Sci. Lett.* 288, 534–538.
- Wade, J., Wood, B.J., 2005. Core formation and the oxidation state of the Earth. *Earth Planet. Sci. Lett.* 236, 78–95.
- Wenk, H.R., Matthies, S., Hemley, R.J., Mao, H.K., Shu, J., 2000. The plastic deformation of iron at pressures of the Earth's inner core. *Nature* 405, 1044–1047.
- Williams, Q., Jeanloz, R., 1990. Melting relations in the iron–sulfur system at ultra-high pressures: implications for the thermal state of the Earth. *J. Geophys. Res.* 95, 19299–19310.